REAL: Research in Education Assessment and Learning ISSN: 1947-5497 www.realjournal.org

Research Article in Empirical Study

Design and Test of a Multi-Axis Acoustic-Levitation Device for Non-Contact Dust Removal from Precision Instruments

Yudi Niu[1], Yifan Pu[2], Xiaoqi Che [3], Hong Gao [3], Mei Wang [3*]

[1] School of Biomedical Engineering, Beihang University, Beijing 100191, China

[2] School of Automation Science and Electrical Engineering, Beihang University, Beijing 100191, China

[3] Department of Physics, Beihang University, Beijing 100191, China

[*] Correspondence: rose@buaa.edu.cn

(Received: 12/18/2019; Accepted: 04/10/2020; Published: 04/22/2020)

DOI: https://doi.org/10.37906/real.2020.3

Abstract: To resolve the issues of the conventional dust removing method, such as electrostatic suspension and direct wiping with special lens paper, which can cause damage to precision instruments and their dependence on specific dust particle properties, we present a novel acoustic-levitation device design which incorporates an initial design of a multi-axis levitation device by Marzo. A. with our enhancement model based on the variation of transducers numbers and their spacing to achieve the dust removing efficiency and feasibility in real dust removal process. In this work, modeling simulation in COMSOL Multiphysics and light absorbance experiment are performed to evaluate the distribution of acoustic fields, trajectory of dust particles, and dust removing efficiency. With the manufactured device based on our design, the varying factors are characterized that may influence the removing efficiency when output voltage generated onto motor driven board is altered. Experiment shows 27.5 V is the most efficient voltage output with highest dust removal proportion in actual removing operations. The study demonstrates our design can achieve higher dust removing efficiency comparing to conventional methods. Whereas our design serves the purpose to solve a practical industrial problem, this paper also shows how it can be taken into the classroom as an demonstration experiment, providing an animated way to visualize the nodes and antinodes by the levitation position of particles, which help the students to not only understand the physical properties of standing waves, but also the connection from a classroom lab to an industrial solution.

Keywords: Acoustic Levitation, Non-Contact Dust Removal, Precision Instrument

Introduction

The widespread use of precision instruments in biology or chemistry experiments demands dust removal operations with high efficiency without direct contacts and potential abrasion. The possible methods for dust removal operations fall into three categories: direct contact wiping (Rauert et al. 2016), applying electrostatic preceptors (Calle et al. 2009), and using a wind blower (Uetake et al. 1999). The first method neglects the fact that in some applications it is highly desirable that the cleaning process does not make physical contact with the surface to be cleaned (Fuhrmann et al. 2013). For instance, the accuracy of the lens of high precision instruments, from microscope to analytical devices of biochemistry test, can be degraded due to cleaning contact. Though the other two methods are noncontact dust removal operations, some problems still exist due to either the limitation towards physical properties of targeted particles (the

chargeability, size, and shape), or the negative interference with electrical instruments from electrostatic preceptors and the failure to collect potentially toxic chemicals within uncontrollable blowing direction of wind blowers, which remain difficult to address. The advantages and disadvantages of conventional dust removal methods and corresponding dust removal efficiency are summarized in Table 1.1 to 1.3. The unsolved challenges stated above reduce the effectiveness, efficacy and safety of dust removal devices, violating preciseness of biology or chemistry experiments.

Table 1.1 Summary of advantages, disadvantages, and operation efficiency of conventional dust removal methods (Lens paper)

Advantages	Disadvantages	Efficiency
● Disposable ● Cheap ● Convenient manual operations	● Possible surface damage ● Reduction in precision of optical precision instrument	Of high manual variation

Table 1.2 Summary of advantages, disadvantages, and operation efficiency of conventional dust removal methods (Wind blower)

Advantages	Disadvantages	Efficiency
● Noncontact	● Failure to achieve orientated collection ● Possible pollution to surrounding environment	Depending on particle sizes, 50% for PM10 (Chen et al. 2015)

Table 1.3 Summary of advantages, disadvantages, and operation efficiency of conventional dust removal methods (Electrostatic precipitator)

Advantages	Disadvantages	Efficiency
● Noncontact ● High removal radius range of particles ● Automatic control	● Dependency on particle residence, temperature and humidity ● High removal efficiency on limited particle types	37 to 79% (Mitchell et al. 2004; Ritz et al. 2006)

To address the issues with existing ultrasound-cleaning devices, this paper presents our attempted optimized design of multi-axial levitation devices with stable levitation force under the impact from a reflective surface during actual cleaning process at a low cost compared to the existing device, utilizing the fact that particles can be trapped in pressure nodes in standing waves owing to a spring action through which particles can be suspended in air (Marzo et al. 2017). Our work starts with coming up with an initial design (denoted as "Initial Design" hereafter in this paper) incorporated from previous studies by Marzo. A. The Initial Design exhibits superior stable levitation forces, and its efficacy is analyzed. By enhancing the Initial Design, we accomplished an optimized design (denoted as "Optimized Design" hereafter in this paper), for which the acoustic field and the trajectory of removable particles are simulated in COMSOL Multiphysics in order to evaluate the levitation effect and to examine the effectiveness. In addition, a spectrophotometer is used to quantitatively analyze the dust removal proportion on a fixed flat area by measuring light absorbance of targeted waste solution. Based on simulation results and considering the potential factors that may alter dust removal performance for a given design, voltage output is selected as an adjustable variable during practical use, and 27.5 V is the attainable ideal voltage output for our enhanced design with highest dust removal efficiency. Our work demonstrates the design of an acoustic levitation device with an optimized set of voltage outputs, validated by simulation and measurement of dust removal properties, which can attain a maximum removal efficiency of 90.4% without causing potential damage to precision instruments, as compared to the conventional dust removal approaches.

Whereas the fabricated acoustic levitation in our design aims to solve a practical industrial problem, it can also be applied in demonstration experiment to help students gain a better understanding of the properties of acoustic standing waves. Firstly, with particles reaching stable levitation, the device can be applied to achieve acoustic visualization and quantitative measurement of distance between nodes and antinodes. Secondly, combining with the estimation of location of nodes and antinodes derived from function of acoustic standing waves, the demonstration experiment based on the design can include small disturbance to the levitated particles which further illustrates the significant properties of acoustic standing waves that the levitation position and fluctuating amplitude is independent of time. Finally, measurement of levitation position can be integrated with the formula of acoustic levitation force to achieve constant fitting which can be taken as an alternative method to measure relatively small particle radius that is hard to obtain.

The rest of the paper is organized as follows. The Initial Design and Optimized Design are described in detail. For the Optimized Design, the simulation in COMSOL Multiphysics (distribution of acoustic fields and the trajectory of targeted particles in the field before the formation of stable acoustic levitation forces to study its dynamic patterns), the light absorbance measurement to determine dust removal efficiency on a specific flat area of precision instruments, and the experimental results are described in detail. Finally the paper addresses how to apply the design in experimental demonstration, and ends with the conclusion.

Initial Design

The Initial Design of acoustic levitation devices is incorporated from the previous work of A. Marzo, et al (Marzo et al. 2017). To achieve the stability of acoustic levitation forces and steady formation of acoustic fields, the original device made use of multi-axial levitation methods, and used an optimized design of curvature radius of the emission surface, on which the ultrasound wave emitters are planted in order to produce the most concentrated acoustic fields. As a result, the particles are restricted to the acoustic traps under stabilized levitation force. A. Marzo used transducers operating at 40 kHz (k¼8.5 mm): 10 mm diameter transducers (MA40S4S) for the Straight Tubes and Coils, and 16 mm diameter transducers for the Sculpted Surface (MCUSD16P40B12RO) (Marzo et al. 2017). The details of the production process are as follows.

Firstly, program an Arduino Nano to generate 4 half-square signals at 5 Vpp 40 kHz with different phases. Signals will be amplified to 25 Vpp by the L298N motor driver, and then enter into the ultrasonic transducers. Then transducers are mounted in a 3D-printed bowl. With a flat reflective surface under the bowl, the bowl's shape focuses the ultrasonic waves in the center of the bowl. Meanwhile, it is desired to locate the actuators in a way that maintains symmetry related behavior to enhance focusing effect. This can be achieved by spacing the actuators equally along the circumference of the annulus in a particular way. For n actuators, the angular spacing between every two actuators would be $\frac{2\pi}{n}$ (Kandemir & Calkan, 2016). A 12 V DC battery powers the Arduino and the logic part of the L298N. A LM2577 DC-DC Converter boosts the voltage into 25 V to the L298N.

The fabricated design is depicted as follows in Fig. 1.

Figure 1: Diagram of the acoustic levitation device (Initial design)

Simulation of Acoustic Fields

Firstly, the spatial arrangement of emitting transducers is determined by three factors in spherical coordinate system: distance from the original point r, and angles of the two axes θ and φ. The formula used below transfers spherical coordinates into Cartesian coordinates in order to set the central point of transducers in spatial area:

$$x = rcos\varphi sin\theta, y = rsin\varphi sin\theta, z = rcos\theta \quad (1)$$

The coordinate of bottom circle's central point of each transducer is defined with a fixed distance of 1 mm. The transducers are made out of aluminum, and the geometry shape is defined as a cylinder with 8 mm in radius and 10 mm in height. Cartesian coordinates using directional vectors determine the directions of each transducer. Radial distribution of the transducers is symmetrical.

The levitation height is controlled by several physical parameters but mostly by the squeeze number, σ (Gabai et al. 2017; Bucher et al. 2016):

$$\sigma = \frac{12\omega\mu_0 L^2}{p_0 {h_0}^2} \tag{2}$$

Secondly, reflective surface is built as a cylinder made of glass (quartz). Parameters of modeling design of reflective surface used in real dust removal operations are as follows: the velocity of sound is 5664 m/s; the medium density is 2210 kg/m3; the thickness is 10 mm; the distance between margin of transducers and reflective surface is 0.5 mm. The medium within the device is air with ϱ (kg/cm3) in density, cs (m/s) in transmission speed, 293.15 K (12) in temperature and 1 atm in pressure.

Thirdly, physical fields in our simulation model are established through simulation of pressure acoustics, fluid model, and plane wave radiation. In the simulation of pressure acoustics, three-dimensional analysis domain is selected to complete the simulation, and initial pressure is set to 0. Due to low density of heat conduction and the pursuit of a simplified model to reduce computational complexity, the fluid model in our simulation process is based on the air which neglects the effect of fluid viscosity and heat conduction within particles and medium. The analytical formulas of fluid model are listed as follows.

$$\nabla \cdot (-\frac{1}{\rho_c}(\nabla p_t - q_d)) - \frac{{k^2}_{eq} p_t}{\rho_c} = Q_m$$
$$p_t = p + p_b,\ k_{eq}^2 = (\frac{\omega}{C_c})^2,\ C_c = C,\ \rho_c = \rho \tag{3}$$

The set of plane wave radiation defines the medium as air on all analytical margins which neglects the influence of other reflective surface. The analytical formula of plane wave radiation analysis is as follows (Kierkegaard et al. 2010).

$$-n \cdot \nabla \cdot (-\frac{1}{\rho_c}(\nabla p_t - q_d)) + i\frac{k_{eq}}{\rho_c} p + \frac{i}{2k_{eq}\rho_c}\Delta_{\parallel} p = Q_i \tag{4}$$

In addition, emitting phase difference of transducers on symmetrical positions is π and pressure on either side is 300 Pa or -300 Pa to guarantee the phase difference.

Fourthly, analytical grids on the model are set as refinement to ensure computational accuracy. Based on the established model in COSMOL Multiphysics, a simulation is performed to analyze the distribution and density of acoustic fields and acoustic isobaric surface.

The experimental parameters of the transducers in the simulation are listed in Table 2.

Table 2: Experimental parameters of the emission surface of transducers in spherical and Cartesian coordinate systems

Spherical coordinate system					Cartesian coordinate system		
r/mm	θ/°	φ/°	θ/rad	φ/rad	x/mm	y/mm	z/mm
50	25	30	0.436332313	0.523598776	18.29990754	10.56545654	45.31538935
50	25	90	0.436332313	1.570796327	1.29443E-15	21.13091309	45.31538935
50	25	150	0.436332313	2.617993878	-18.29990754	10.56545654	45.31538935
50	25	210	0.436332313	3.665191429	-18.29990754	-10.56545654	45.31538935
50	25	270	0.436332313	4.71238898	-3.88328E-15	-21.13091309	45.31538935
50	25	330	0.436332313	5.759586532	18.29990754	-10.56545654	45.31538935
50	50	15	0.872664626	0.261799388	36.99710558	9.913344564	32.13938048
50	50	45	0.872664626	0.785398163	27.08376102	27.08376102	32.13938048
50	50	75	0.872664626	1.308996939	9.913344564	36.99710558	32.13938048
50	50	105	0.872664626	1.832595715	-9.913344564	36.99710558	32.13938048
50	50	135	0.872664626	2.35619449	-27.08376102	27.08376102	32.13938048
50	50	165	0.872664626	2.879793266	-36.99710558	9.913344564	32.13938048
50	50	195	0.872664626	3.403392041	-36.99710558	-9.913344564	32.13938048
50	50	225	0.872664626	3.926990817	-27.08376102	-27.08376102	32.13938048
50	50	255	0.872664626	4.450589593	-9.913344564	-36.99710558	32.13938048
50	50	285	0.872664626	4.974188368	9.913344564	-36.99710558	32.13938048
50	50	315	0.872664626	5.497787144	27.08376102	-27.08376102	32.13938048
50	50	345	0.872664626	6.021385919	36.99710558	-9.913344564	32.13938048
50	75	10	1.308996939	0.174532925	47.56256213	8.386562975	12.94095226
50	75	30	1.308996939	0.523598776	41.82581519	24.14814566	12.94095226
50	75	50	1.308996939	0.872664626	31.04425765	36.99710558	12.94095226
50	75	70	1.308996939	1.221730476	16.51830448	45.38366856	12.94095226
50	75	90	1.308996939	1.570796327	2.95851E-15	48.29629131	12.94095226
50	75	110	1.308996939	1.919862177	-16.51830448	45.38366856	12.94095226
50	75	130	1.308996939	2.268928028	-31.04425765	36.99710558	12.94095226
50	75	150	1.308996939	2.617993878	-41.82581519	24.14814566	12.94095226
50	75	170	1.308996939	2.967059728	-47.56256213	8.386562975	12.94095226
50	75	190	1.308996939	3.316125579	-47.56256213	-8.386562975	12.94095226
50	75	210	1.308996939	3.665191429	-41.82581519	-24.14814566	12.94095226
50	75	230	1.308996939	4.01425728	-31.04425765	-36.99710558	12.94095226
50	75	250	1.308996939	4.36332313	-16.51830448	-45.38366856	12.94095226
50	75	270	1.308996939	4.71238898	-8.87552E-15	-48.29629131	12.94095226
50	75	290	1.308996939	5.061454831	16.51830448	-45.38366856	12.94095226
50	75	310	1.308996939	5.410520681	31.04425765	-36.99710558	12.94095226
50	75	330	1.308996939	5.759586532	41.82581519	-24.14814566	12.94095226
50	75	350	1.308996939	6.108652382	47.56256213	-8.386562975	12.94095226

Simulation of Particles' Trajectory

To simulate the particles trajectory for the purpose of analyzing the stability of acoustic levitation device that transports dust particles, Fluid Particle Trajectory (FPT) is used for this purpose. The boundary condition of wall 1 (air) is disappearance of boundary condition, and the particles is defined as 500 kg/m^3 (Becklin et al. 1982) in density and 0.1 mm (Gunnlaugsson et al. 2005) in the diameter of particles. The boundary condition of wall 2 (transducers and reflective surface) is the attachment which serves as the limitation to particles movement trajectory on the border. Apart from the acoustic levitation force, gravitational field is applied to the universal coordinate system as particles are affected by the gravity vector $-\vec{g}$ on the universal scale. Drag forces of stokes equation are used to determine dynamic viscosity of particles. Thus, the computational process can be accomplished based on stated procedures above.

Optimized Design and Experimental Apparatus

The optimized design is an enhancement to the Initial Design based on the improved distribution of transducers with variety in numbers and intervals.

Based on the distribution of transducers in the initial design, we discovered that the 6 transducers on the top of the emission surface are absent. The optimized design is developed in theory to figure out whether the levitation stability will be improved if the 6 transducers are added on the top of the device with simulation done in COMSOL Multiphysics to analyze the distribution of acoustic fields within the new design. This enhancement in the paper is defined as OD.1.

Measurement of Light Absorbance

To test the effectiveness of dust removal operations, we use the measurement of the light absorbance of particle-deionized water solution with dust particles collected from surface of precise instruments before and after removal operations with acoustic levitation device. This measurement evaluates the dust removal efficiency under different voltage output. The experimental equipment used for LAM analysis and measurement of voltage output includes: a visible spectrophotometer (V-5100B), a vortex oscillator, a 1000 μm pipette, cuvettes, burettes, and universal meter.

A square of 1 cm^2 curved on acrylic plate is defined as the targeted range for dust removal operation. 0.1 g of sawdust is evenly placed on the area at the start of each removal operation. Acoustic levitation device is set approximately 1 cm above the plate surface. To avoid disturbance of air within the bowl caused by acoustic levitation forces, the dust removal operation is not started on top of the ideal dust removal area. After proper alignment, the device is activated to complete the operation with artificial control over the motion trajectory after the stable levitation of particles is formed. To quantitatively analyze the efficiency of dust removal operation, we defined the effective dust removal operation as the collection from limited area (1 cm^2 square curved as formerly demonstrated) and successful transportation to the ideal area which symbolizes the controllable dust removal operation compared to conventional dust removal methods.

The removed quantity of sawdust is measured by the reduced light absorbance within deionized water. The remaining sawdust on the control area is collected and tested through light absorbance measurement after each dust removal operation at different voltage output ranging from 15 V to 30 V at the interval of 2.5 V. The dust removal efficiency at different voltage output is calculated to find the optimized performance of acoustic levitation device by the following formula, where a is dust removal efficiency; d is initial light absorbance; d' is light absorbance of remaining sawdust; ω_0 is light absorbance of deionized water:

$$a = \frac{(d - w_0) - (d' - w_0)}{d - w_0} \times 100\% \tag{5}$$

Experimental Results

The experimental results to test the effectiveness of OD.1 including the simulation results from COMSOL Multiphysics and the light absorbance measurement (LAM) results (Petzold & Schönlinner, 2004) are shown below.

Simulation Results of COMSOL Multiphysics

Distribution of the Acoustic Field

The color of the acoustic field in our simulation model represents the density of acoustic fields. Red indicates the high density while blue represents the low density. The stable levitation is formed between acoustic potential well within higher density acoustic field and lower density acoustic field.

Simulation results of initial design and optimized design (OD.1) are shown in Fig. 2 and Fig. 3.

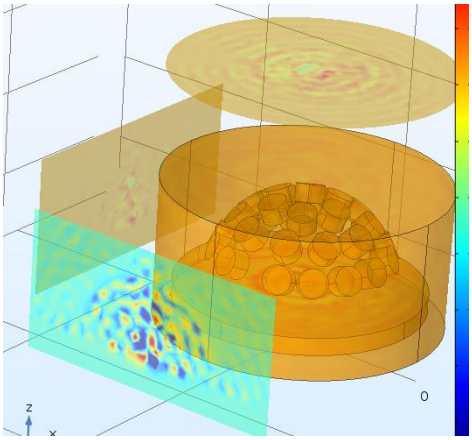

Figure 2: Simulation results of acoustic field within optimized design (OD.1)

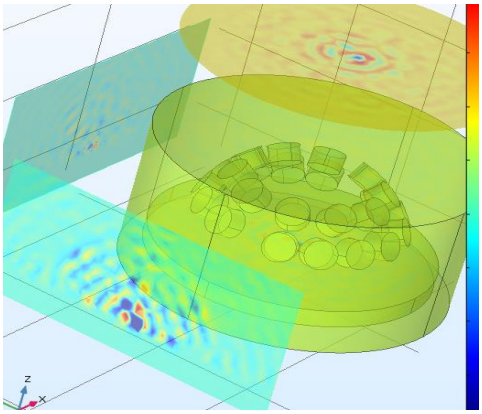

Figure 3: Simulation results of acoustic field within initial design

Figure 2 and 3 are shown at the same scale to compare the density of acoustic fields, which represents the capability of levitation device to control the levitation stability of dust particles. Due to the levitation forces produced by the transducers on top of the emitting surface, the area within the top shows a significant pattern in the increasing of density of acoustic field. Relatively more acoustic potential wells with higher density are seen at the bottom of the device which is adjacent to the reflective surfaces, indicating the enhancement of levitation capability near the reflective surfaces during dust removal operations.

However, given that the dust particles are levitated between the traps formed by acoustic fields of high and low density, and the numbers of acoustic traps formed by optimized design near the surface show no sign of significant variation compared to the initial design, we conclude that although the density of acoustic fields increase significantly within the top of the device with transducers added in the OD.1, the levitation forces are of little difference around the targeted plate surface compared to the initial design at the efficacy of levitating dust particles. In addition, the addition of 6 transducers on the top gives rise to the

consumption of more electricity power, which eliminates the functioning time after each charging which violates the initial goal of designing a dust removing acoustic levitation device of great convenience.

Thus, considering both factors, the significance in the increase of density in acoustic fields adjacent to the reflective surface and the convenience of using the dust removing device with higher working efficacy and lower electrical power consumption, we concluded that the initial design is indeed the more efficient design that is supported by the analysis towards density of acoustic fields in COMSOL Multiphysics computational results.

Movement Trajectory of Dust Particles

Based on the previous simulation of the density of acoustic fields, the initial design is proved as a more efficient design which guarantees the relatively stable levitation forces and high density of acoustic fields at the low cost of transducers use. Therefore, the initial design is selected as the ideal levitation device during dust removal process and movement tack of dust particles at the diameter of 0.1 mm, testing the gathering condition of dust particles within the devices through simulation which is hard to observe during real dust removal process due to the close distance between the device and targeted dust removal surface. We performed a simulation to explain the dynamics of dust particles before stable acoustic levitation while LAM analysis serves as the quantitative evidence to analyze the dust removal efficiency in actual removing process.

The simulation results are shown in Fig. 4 as follows (The simulation results are based on dynamic trajectory changes, while the figure below shows the condition with the highest degree of particle aggregation at stable acoustic levitation.)

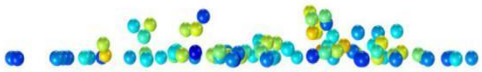

Figure 4: Simulation of dust particle trajectories at the moment with highest degree of particle aggregation

LAM Analysis at Different Voltage Output

The dust removal operation reaches the highest efficiency of 90.4% at the output voltage of 27.5 V. The result of LAM analysis indicates the voltage output is a factor that is easy to change and control after device fabrication, thus the efficient target can be met during dust removal operations. The efficiency of dust removal operations at different voltage output is calculated based on equation (4), and is shown in Fig. 5 as follows.

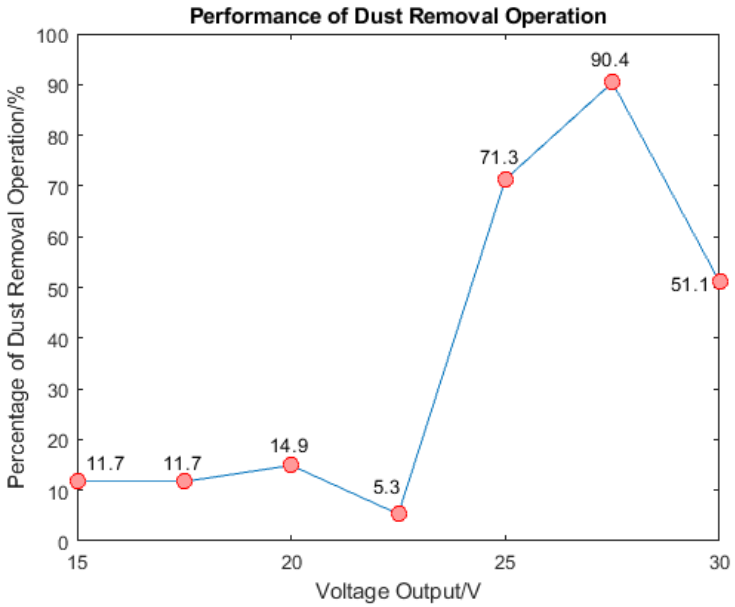

Figure 5: Performance of dust removal operation at different voltage output

Discussion

Reduction in dust removal efficiency

In the actual dust removal process, we found that the dust particles were levitated or blown away within the starting interval of the activation of levitation device. The simulation was performed to analyze the trajectory of dust particles, and the results show the consistent conditions. This indicates the possibility of potential reduction of targeted particles and elimination in dust removal efficiency. The movement trajectory of dust particles at the beginning before the formation of stable acoustic fields is shown in Fig. 6.

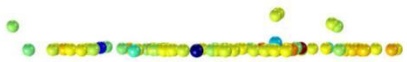

Figure 6: Simulation of trajectories within the starting interval of activation of levitation device before the formation of stable acoustic fields

Therefore, one possible improvement of current design is the elimination of particle blowing and reduction before the formation of stable acoustic fields to guarantee a higher removing efficiency by enhancing acoustic focusing effect.

Application in demonstration experiment

The levitation device can also be applied in demonstration experiment to help validate understanding of physical properties of standing waves and acoustic radiation forces.

Assume time starts at particle at x=0 when it reaches the maximum displacement, positive direction is along x axis, the incident wave function and reflected wave function can be respectively described as following functions:

$$y_1 = dcos2\pi(ft - \frac{x}{\lambda}), y_2 = dcos2\pi(ft + \frac{x}{\lambda}) \quad (6)$$

where d is amplitude, f is frequency, and λ is wavelength.

The superposed standing wave function can be further described as follows:

$$y = y_1 + y_2 = 2dcos2\pi ft \cdot cos2\pi \frac{x}{\lambda} \quad (7)$$

We can obtain that fluctuating particles fluctuates at the same frequency and the amplitude which equals to $\left|2dcos2\pi \frac{x}{\lambda}\right|$, which is independent of time and only defined by the location of particles.

Furthermore, the location of fluctuating particles at nodes and antinodes can be calculated. Position of nodes is $x_{node} = (2k+1)\frac{\lambda}{4}$ and position of antinodes is $x_{antinode} = k\frac{\lambda}{2}$. As a result, distance between neighboring nodes or antinodes is $\Delta x = x_{k+1} - x_k = (2(k+1)+1)\frac{\lambda}{4} - (2k+1)\frac{\lambda}{2} = \frac{\lambda}{2}$.

Based on the experimental analysis, the distance between stable levitation points of particles within the device equals Δx. Thus, the device can achieve the visualization of acoustic field, and be used as a portable device to measure the wavelength of ultrasound and estimate the frequency.

The amplitude of a certain fluctuating point is dependent on the position of particles. Thus, the propagation of standing wave does not include fluctuating patterns within particles at different locations and vibration energy. When a particle has reached stable levitation status, the levitation position will not change in time, and will return to the initial state under slight perturbation. This device can be included in demonstration experiment to help students grasp a better understanding of physical properties of standing waves.

Assume that the geometry size of rigid ball in acoustic levitation field is much smaller than the wavelength, the scattering effect can be neglected and acoustic levitation force can be described as follows (Bruus, 2012):

$$f = -\frac{4\pi R^3}{3}\rho_0 k A^2 \sin(2kx) \quad (8)$$

At positions of antinodes where particles reach stable levitation, the acoustic levitation force reaches maximum value. Thus, during experiments, adjustment to acoustic properties can be combined with this theoretical equation to achieve successful levitation of particles with different sizes and densities. Besides, with known mass of the particle and properties of acoustic field, different levitation location can be recorded for fitting of the equation for acoustic levitation force and thus achieve measurement of the particle radius.

Limitations

As a preliminary study, impact of other experimental factors that can possibly affect dust removal efficiency, such as distance between transducers, oriented position of transducers, and frequencies of ultrasound, are not fully studied. The interaction between levitated particles and acoustic field and corresponding changes in acoustic forces are neglected during numerical simulation, based on the assumption that the geometry size of particles is much smaller than wavelength. Although the dust removal efficiency is quantitatively verified by LAM, the collection and artificial transportation of sawdust during measurement process can cause reduction, and is varied between different operators.

Conclusion

In conclusion, this paper presents an acoustic-levitation device with Initial Design and our Optimized Design. Simulation and experimental measurements finds that the initial design is a device with high density in acoustic fields near the targeted dust removal surface using fewer transducers as compared to the optimized design (OD.1). A voltage of 27.5 V is the most efficient voltage output for the highest dust removal proportion in actual removing operations once the design is manufactured and the corresponding acoustic parameter cannot be altered. The trajectory of dust particles at the beginning indicates that in order to enhance dust removal efficiency, future improvements of acoustic levitation design can be done to increase the acoustic focusing effect by changing the position of transducers after the activation of device. Whereas the design serves to solve an industrial problem, it can be applied in classroom as an experimental demonstration as well.

Funding: This research was funded by National Natural Science Foundation of China (Work function modulation of TiLixOy/Graphene/SiC stack and controllability of its memristive behaviors, grant number 11574017")

Acknowledgments: The scientific contributions is provided by Basic Physics Experimental Laboratory, School of Biomedical Engineering and School of Automation Science and Electrical Engineering in Beihang University of Astronautics and Aeronautics.

Conflicts of Interest: The authors declare no conflict of interest." The funders had no role in the design of the study; in the collection, analyses, or interpretation of data; in the writing of the manuscript, or in the decision to publish the results".

References

Rauert, C., Kuribara, I., Kataoka, T., Wada, T., Kajiwara, N., Suzuki, G., ... & Harrad, S. (2016). Direct contact between dust and HBCD-treated fabrics is an important pathway of source-to-dust transfer. Science of The Total Environment, 545, 77-83.

Calle, C. I., Buhler, C. R., McFall, J. L., & Snyder, S. J. (2009). Particle removal by electrostatic and dielectrophoretic forces for dust control during lunar exploration missions. Journal of Electrostatics, 67(2-3), 89-92.

Uetake, H., Nakagawa, J., Horota, N., & Kitazawa, K. (1999). Nonmechanical magnetothermal wind blower by a superconducting magnet. Journal of applied physics, 85(8), 5735-5737.

Fuhrmann, A., Marshall, J. S., & Wu, J. (2013). Effect of acoustic levitation force on aerodynamic particle removal from a surface. Applied Acoustics, 74(4), 535-543.

Chen, Shuwen, et al. "Self-powered cleaning of air pollution by wind driven triboelectric nanogenerator." Nano Energy 14 (2015): 217-225.

Mitchell, B. W., Richardson, L. J., Wilson, J. L., & Hofacre, C. L. (2004). Application of an electrostatic space charge system for dust, ammonia, and pathogen reduction in a broiler breeder house. Applied Engineering in Agriculture, 20(1), 87.

Ritz, C. W., et al. "Improving in-house air quality in broiler production facilities using an electrostatic space charge system." Journal of applied poultry research 15.2 (2006): 333-340.

Marzo, A., Ghobrial, A., Cox, L., Caleap, M., Croxford, A., & Drinkwater, B. W. (2017). Realization of compact tractor beams using acoustic delay-lines. Applied Physics Letters, 110(1), 014102.

Kandemir, M. H., & Çalışkan, M. (2016). Standing wave acoustic levitation on an annular plate. Journal of Sound and Vibration, 382, 227-237.

R. Gabai, D. Ilssar, R. Shaham, N. Cohen, I. Bucher, A rotational traveling wave based levitation device - modelling, design, and control, Sensor Actuat. A: Phys. 255 (2017) 34 – 45.

Bucher, I., Ilssar, D., Gabai, R., Cohen, N., Shaham, R., & Davis, S. (2016, July). Controlled acoustic levitation----physical model and real-time digital implementation. In Advanced Intelligent Mechatronics (AIM), 2016 IEEE International Conference on (pp. 452-456). IEEE

Vandaele, V., Lambert, P., & Delchambre, A. (2005). Non-contact handling in microassembly: Acoustical levitation. Precision engineering, 29(4), 491-505.

Kierkegaard, A., Boij, S., & Efraimsson, G. (2010). A frequency domain linearized Navier–Stokes equations approach to acoustic propagation in flow ducts with sharp edges. The Journal of the Acoustical Society of America, 127(2), 710-719.

Becklin, E. E., Gatley, I., & Werner, M. W. (1982). Far-infrared observations of Sagittarius A-The luminosity and dust density in the central parsec of the Galaxy. The Astrophysical Journal, 258, 135-142.

Gunnlaugsson, T., Kruger, P. E., Jensen, P., Tierney, J., Ali, H. D. P., & Hussey, G. M. (2005). Colorimetric "naked eye" sensing of anions in aqueous solution. The Journal of organic chemistry, 70(26), 10875-10878.

Petzold, A., & Schönlinner, M. (2004). Multi-angle absorption photometry—a new method for the measurement of aerosol light absorption and atmospheric black carbon. Journal of Aerosol Science, 35(4), 421-441.

Bruus, H. (2012). Acoustofluidics 7: The acoustic radiation force on small particles. Lab on a Chip, 12(6), 1014-1021.